

Novel formulation, cytotoxicity, antioxidant, and anti-human lung cancer properties of gold nanoparticles containing *Verbascum thapsus* L. leaf aqueous extract

Kaijin Lu¹, Yan Ou², Lihao Jiang³, Yijia Xiao⁴, Arunachalam Chinnathambi⁵, Tahani Awad Alahmadi⁶, Milton Wainwright⁷

¹Department of Thoracic Surgery, Taizhou People's Hospital of Jiangsu Province, Taizhou city, Jiangsu Province, China

²Respiratory Medicine, Chongqing Armed Police Corps Hospital, Chongqing, China

³Department of Oncology, The People's Hospital of Dazu, Chongqing, China

⁴Department of Respiratory and Critical Care Medicine, Changsha Central Hospital of Hunan Province, Changsha, Hunan, China

⁵Department of Botany and Microbiology, College of Science, King Saud University, Riyadh, Saudi Arabia

⁶Department of Pediatrics, College of Medicine and King Khalid University Hospital, King Saud University, Medical City, Riyadh, Saudi Arabia

⁷Department of Molecular Biology and Biotechnology, University of Sheffield, Sheffield, UK

Corresponding author:

Yijia Xiao

Department of Respiratory

and Critical Care Medicine

Changsha Central Hospital

of Hunan Province

Changsha, Hunan

China

E-mail: xiaoyijia121@sina.com

com

Submitted: 29 July 2021; **Accepted:** 7 August 2021

Online publication: 17 August 2021

Arch Med Sci

DOI: <https://doi.org/10.5114/aoms/141043>

Copyright © 2021 Termedia & Banach

Abstract

Introduction: In the present study, gold nanoparticles were prepared and synthesized in aqueous medium using *Verbascum thapsus* leaf extract. We assessed the anti-human lung cancer potential of these nanoparticles against well-differentiated bronchogenic adenocarcinoma, moderately differentiated adenocarcinoma of the lung, and poorly differentiated adenocarcinoma of the lung cell lines.

Material and methods: AuNPs were characterized and analyzed by common nanotechnology techniques including Fourier transform infrared (FT-IR) and ultraviolet-visible (UV-Vis) spectroscopy, field emission-scanning electron microscopy, and transmission electron microscopy. In the FT-IR test, the presence of many antioxidant compounds with related bonds caused excellent conditions for reduction of gold in the gold nanoparticles. In UV-Vis, the clear peak at the wavelength of 548 nm indicated the formation of gold nanoparticles. For determining anti-human lung cancer properties of HAuCl₄, *V. thapsus*, and AuNPs, MTT assay was used on normal (HUVECs), well-differentiated bronchogenic adenocarcinoma (HLC-1), moderately differentiated adenocarcinoma of the lung (LC-2/ad), and poorly differentiated adenocarcinoma of the lung (PC-14) cell lines.

Results: AuNPs had excellent anti-human lung cancer effects dose-dependently against HLC-1, LC-2/ad, and PC-14 cell lines. The best result of anti-human lung cancer activities of AuNPs against the above cell lines was observed in the case of the PC-14 cell line.

Conclusions: The synthesized AuNPs showed significant anti-human lung cancer properties against well-differentiated bronchogenic adenocarcinoma, moderately differentiated adenocarcinoma of the lung, and poorly differentiated adenocarcinoma of the lung cell lines in a dose-dependent manner.

Key words: gold nanoparticles, *Verbascum thapsus* L., lung well-differentiated bronchogenic adenocarcinoma, lung moderately differentiated adenocarcinoma, lung poorly differentiated adenocarcinoma.

Introduction

Cancer is a genetic disease that includes 277 types of diseases. There are also more than 100,000 types of chemicals in our environment, of which only 35,000 have been analyzed and about 300 of them cause cancer. The remaining 65,000 chemicals in nature have not yet been tested. Cancer occurs due to uncontrolled cell division, which is the result of environmental factors and genetic disorders [1–3]. The four key genes involved in cancer cell conduction are DNA repair genes, tumor suppressor genes, oncogenes, and programmed death genes [2, 3]. If a genetic mutation is produced in a cell, normal cells go out of their way and are affected by new commands that progress to cancer cells. In addition to chemicals, sunlight, shortwave radiation, viruses and bacteria also have a special role in causing cancer [4, 5]. Cancers have existed since the beginning of mankind. In recent decades, advances in computer molecular medicine have been able to not only study the causes and mechanisms of this deadly disease but also to perform better in its early diagnosis and treatment [5–7]. More than 50% of cancers are currently being treated, especially if diagnosed early. Cancer can be treated in several ways: surgery, chemotherapy, radiation therapy, immunotherapy, gene therapy, or a combination of these. Due to the relative inefficiency and very severe side effects of chemotherapeutic drugs, researchers and scientists have sought a new formulation of various compounds, especially metallic nanoparticles [2–5].

In recent decades, the application of nanotechnology has played an important role in the development of science. Nanoscience has shown that if we reduce the size to nanometers, unique properties such as optical properties, electrical conductivity, hardness, and chemical reaction will be obtained. Nanoparticles are widely used because of their high surface-to-volume ratio, small size, and excellent reactivity. One of the most important advances in nanotechnology is the production and application of nanoparticles in the biological sciences [5–7]. Nanoparticles are generally effective in a wide variety of sectors; if their production is based on green chemistry, they have great applications in the fields of food, medicine, cosmetics and health. Nanoparticles centered on inorganic materials such as magnetic metals, their oxides and alloys, and semiconductors have the most studies and potential in biomedicine from diagnosis to treatment of diseases [7–9]. The effects of nanoparticles should be predictable, controllable and get the desired results with minimal toxicity. Metallic nanoparticles used in treatment and diagnosis, in addition to being non-toxic, must be biocompatible and stable *in vivo*. Also, by mak-

ing appropriate changes in the surface of metallic nanoparticles, they will have a wide range of applications by binding to biomolecules and various carriers to cross the cell membrane and target the desired part of the body. One of the important points in the production of nanoparticles is the use of cost-effective and efficient precursors [10–12]. There are three methods to synthesize nanoparticles: biological, chemical, and physical. Chemical and physical methods are time-consuming and costly. In addition, these methods use some toxic additive chemicals that cause adverse effects on medical applications by adsorption on the surface. Applying the principles of green chemistry has decreased the use of toxic compounds or hazardous solvents, provided optimal regeneration conditions and ameliorated materials for the chemical processes, and raised new sources for green synthesis [13–16]. Therefore, one of the primary goals of green nanotechnology is to produce nanomaterials without harm to human health or the environment, and to develop and design nanomaterials and products that are suitable solutions to environmental problems. The synthesis of nanoparticles by similar biological methods results in greater catalytic activity and limits the use of toxic and expensive chemicals. In biological methods, plant extracts, enzymes or proteins carrying natural resources are used to produce or stabilize nanoparticles. The nature of the materials used to make nanoparticles influences the shape, structure and morphology of these nanoparticles [16–18]. Biological systems are involved in the green synthesis of nanoparticles, plants and their derivatives, as well as microorganisms such as algae, fungi, and bacteria. Plant parts such as roots, leaves, stems, fruits, and tiny parts such as the kernel and skin of the fruit are suitable to synthesize the nanoparticles because their extracts are rich in phytochemicals that act as stabilizing and reducing substances [6, 8]. The use of natural plant extracts is a cheap and environmentally friendly process and does not require intermediate groups. Short time, no need for expensive equipment, precursors, high purity product and excellent quality without impurities are the features of this method. This is possible very quickly, at room temperature and pressure as well as easily on a large scale. Bio-reduction in the conversion of base metal ions is carried out by various plant metabolites such as alkaloids, phenolic compounds, terpenoids and coenzymes [15–19].

Recently, scientists have used the anticancer effects of medicinal plants in several traditional medicines for synthesizing gold nanoparticles containing natural compounds. So far, the anticancer effects of *Tinospora cordifolia*, *Sophora subprostrata*, *Euphoria hirta*, *Barleria prionitis*, *Lupinus perennis*, *Maytenus boaria*, *Cephaelis acuminata*,

Phyllanthus niruri, *Solanum seaforthianum*, *Boswellia serrate*, *Lavandula officinalis*, and *Cephalotaxus harringtonia* drupacea have been proved [19]. One of these plants is *Verbascum thapsus* L. In traditional medicine, *V. thapsus* is used for the treatment of tuberculosis, skin diseases, bruises, piles, frostbites, wounds, cuts, edema, swelling, inflammatory ailments in the respiratory tract, urinary disease, fever, bleeding of lungs and bowel, rectal prolapse, gastrointestinal system ailments, diabetes, diarrhea, dysentery, infectious diseases, and especially lung diseases [20]. It has chemical antioxidant components including β -carotene, lutein, zeaxanthin, cryptoxanthin, triterpene A, triterpene B, saikogenin A, veratric acid, β -spinasterol, 6-O- β -D-xylopyranosyl aucubin, thapsuine B, hydroxythapsuine thapsuine A, 3-O-fucopyranosyl-saikogenin F, α -tocopherol, γ -tocopherol, and δ -tocopherol [20]. Probably, the remedial properties of this species are related to the above compounds.

In the present research, we decided to investigate the anti-human lung cancer effects of gold nanoparticles formulated by *V. thapsus* against well-differentiated bronchogenic adenocarcinoma, moderately differentiated adenocarcinoma of the lung, and poorly differentiated adenocarcinoma of the lung cell lines.

Material and methods

Material

All materials used in the present study were obtained from Sigma-Aldrich (USA).

Synthesis of AuNPs

First, the leaves of the *V. thapsus* plant, after drying in the air, are pulverized using an electric grinder (model, Moulinex AR1066Q). 25 g of the leaves were soaked by maceration with distilled water and kept for at least 3 days with repeated stimulation to dissolve the solvent at room temperature. After 3 days, the mixture of extract and water was filtered using filter paper to separate the solids from the liquid. Finally, the excess solvent was evaporated and concentrated using a rotary evaporator. With the help of a freezer dryer (Scientific LTE UK, Ltd), it was completely dried and turned into a powder. Finally, the dry powder was stored in a sealed glass container and refrigerated and used to prepare different concentrations [6, 7].

The green synthesis of the AuNPs was initiated with a reaction mixture of 100 ml of $\text{HAuCl}_4 \times \text{H}_2\text{O}$ in the concentration of 1×10^{-3} M and 200 ml of aqueous extract solution of *V. thapsus* leaf (20 $\mu\text{g}/\text{ml}$) in the proportion 1 : 10 in a conical flask (Figure 1). The reaction mixture was kept under magnetic stirring for 12 h at room tempera-

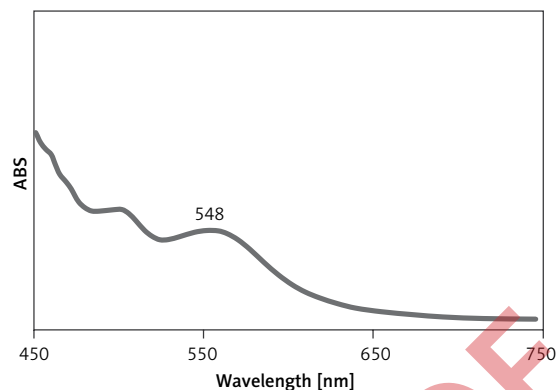


Figure 1. UV-Vis spectrum of biosynthesized gold nanoparticles

ture. At the end of the reaction time, the dark red colored colloidal solution of Au was formed. The mixture was centrifuged at 10 000 rpm for 15 min. The precipitate was washed three times with water and subsequently centrifuged [6, 7]. For analyzing AuNPs, the common techniques of organic chemistry, i.e. FT-IR and UV-Vis spectroscopy, FE-SEM, and TEM were used. AuNPs were primarily confirmed using UV-Vis spectroscopy at a scan range of 450–750 nm wavelength (Jasco V670 Spectrophotometer). The biomolecules involved in the reduction of AuNPs were detected by the FT-IR spectrophotometer (Shimadzu IR affinity.1). The morphological features in terms of shape and sizes were analyzed by FE-SEM (Fe-SEM ZEISS EVO18) and TEM (TEM FEI-TECNAI G2-20 TWIN) microscopic techniques.

Assessment of antioxidant potential of AuNPs by DPPH

Free radicals are unstable atoms that have one or more unpaired electrons. These active species are very harmful due to their high reactivity. They are most often formed when oxygen molecules in the body split into separate unstable atoms. This process can turn into a chain reaction. Excessive production of free radicals in the body causes cell damage and oxidative stress. Genetics and the environment affect the extent of free radical damage in individuals. These active molecules are produced as part of the body's natural biological processes. One of the most important free radicals is DPPH. DPPH is widely used to study the antioxidant activities of natural compounds and nanoparticles [21, 22].

In this method, the antioxidant activity of nanoparticles is measured for DPPH radical scavenging. The basis of the action is the reduction of the alcoholic solution of DPPH in the presence of hydrogen-giving antioxidants, especially phenolic compounds. To achieve the IC_{50} of the samples, 11 different concentrations of nanoparticles were

prepared and the percentage inhibition versus concentration was plotted. In practice, 300 μl of 1 M DPPH was combined with 100 μl of diluted sample to a final volume of 2 ml using methanol. After 0.5 h in the dark, the absorbance was read at 517 nm and the inhibitory percentage was obtained using the following formula:

$$\text{Inhibition (\%)} = \frac{\text{Sample A.}}{\text{Control A.}} \times 100$$

In this formula, "Control A" shows the negative control of light absorption that lacks nanoparticles, and "Sample A" expresses the amount of light absorption of different concentrations of nanoparticles [21, 22].

Measurement of cell toxicity of AuNPs

Investigation of cell proliferation and survival is one of the most important and basic techniques in cell laboratories. This study requires accurate quantification of the number of living cells in the cell culture medium. Therefore, cell survival calculation methods are necessary to optimize cell culture conditions, evaluate cell growth factors, detect antibiotics and anticancer drugs, evaluate the toxic effects of environmental pollutants, and study apoptosis. Many methods can be used for such purposes, but indirect methods using fluorescent or dye (chromogenic) markers provide very fast large-scale methods. Among these methods, measurement of cell survival by the MTT method (3-(4,5-dimethylthiazol-2-yl)-2,5-diphenyltetrazolium bromide) is the most widely used method. This method is a colorimetric method to study cell proliferation and survival, introduced in 1983 by Mossman. The method basis is based on mitochondrial activity. Mitochondrial activity in living cells is stable and therefore a rise or reduction in the number of living cells is linearly related to mitochondrial activity [23]. MTT tetrazolium dye is revived in active cells. Mitochondrial dehydrogenases in living cells break the tetrazolium ring and yield NADPH and NADH, leading to formation of a purple insoluble deposit called formazan. This precipitate can be dissolved by dimethyl sulfoxide or isopropanol. On the other hand, dead cells do not have this ability and therefore do not reveal a signal. Dye formation is used as a marker of living cells. The color intensity produced is measured at a 540 to 630 nm wavelength and is directly proportional to the number of living cells. High safety and providing a colorimetric and non-radioactive system are important advantages of this method. This kit is very easy to use, has high sensitivity and accuracy and can detect less than 950 cells. On the other hand, it has high efficiency for measuring cell proliferation, survival and mortality, and its implementation method does not require time-consuming wash-

ing steps and transfer from one plate to another. Examples studied in this method are adhesive or suspended cells and proliferating or non-proliferating cells [23].

In this experiment, the following cell lines have been used for investing the cytotoxicity and anti-human lung cancer effects of the HAuCl_4 , *V. thapsus*, and AuNPs using an MTT assay:

- 1) Normal cell line: HUVEC.
- 2) Well-differentiated bronchogenic adenocarcinoma cell line: HLC-1.
- 3) Moderately differentiated adenocarcinoma of the lung cell line: LC-2/ad.
- 4) Poorly differentiated adenocarcinoma of the lung cell line: PC-14.

Because nanoparticles are not soluble directly in 1640-RPMI medium and also the solvent of dimethyl sulfoxide nanoparticles (DMSO) itself has cytotoxic effects, to eliminate the effect of this substance on treated cells, its amount in the final solution is considered less than 1%. Dimethyl sulfoxide is not toxic to concentrations less than 1% and the concentration of this solvent is important in this regard. For this purpose, 1000 μg of nanoparticles were dissolved in 100 μl of dimethyl sulfoxide solvent after weighing. Then 1 ml of culture medium was added for better dissolution and finally the volume of solution was increased to 24 ml using culture medium. Then, successive dilutions of this stock were used in the proportions of 1–1000 $\mu\text{g}/\text{ml}$. Eleven concentrations were used for the cell lines [23].

In this study, 100 μl of culture medium containing 10^4 cells per plate 96 were placed. After 24 h, concentrations of 1–1000 $\mu\text{g}/\text{ml}$ of nanoparticles were added to the cells, and incubated for 24, 48, and 72 h, respectively. After these times, 20 μl of MTT plate with a concentration of 5 mg/ml was added to each cell and incubated in the dark for another 4 h. After some time, the MTT medium was carefully removed, and 200 μl of acidified isopropanol was added to each plate to remove the purple formazan. After 15 min of incubation at room temperature, the light absorption of each well was read using an ELISA at 570 nm against a reference wavelength of 690 nm. The findings were reported as cell survival and IC_{50} (concentration that inhibits cell growth up to 50%) based on the concentration curve ($\mu\text{g}/\text{ml}$) [23].

It should be noted that the effect of each concentration of the nanoparticles on cell lines was investigated in five independent experiments. According to the values of light absorption obtained by the ELISA reader, the percentage of growth inhibition related to each concentration was calculated using the following formula:

$$\text{Cell viability (\%)} = \frac{\text{Sample A.}}{\text{Control A.}} \times 100$$

Finally, linear regression was done to determine IC_{50} , which indicates the nanoparticle concentration which causes 50% cancer cell growth inhibition. Using the curve, the linear equation for cancer cells was obtained, then by replacing 50% inhibition in the equation, the IC_{50} value for cancer cells was obtained [23].

Statistical analysis

SPSS statistical software version 22 was used for data analysis and the findings were determined as the mean standard deviation of 5 replications. Data were analyzed using one-way analysis of variance and the Duncan post hoc test and the significance level in the test was considered to be 0.05.

Results and discussion

Recently, the anti-angiogenic and anti-cancer properties of gold nanoparticles have been determined and the findings have revealed that gold nanoparticles can be used as a unique anti-cancer supplement. But the organic solvents used to produce these nanoparticles are toxic and can have devastating environmental effects. Hence there is a great tendency to use healthy methods for synthesizing gold nanoparticles. Recently, studies have begun under the title Green Chemistry, which seeks an environmentally friendly way for nanoparticle synthesis [24–26]. In recent years, gold nanoparticles have been synthesized extracellularly using various plant and microbial extracts. In addition, many studies are underway to investigate the antibacterial, antioxidant and anti-tumor properties of these natural products [25, 26]. In this regard, a study assessed the antibacterial activities of gold nanoparticles synthesized biologically [26, 27]. Another study evaluated the anticancer, antibacterial, and antioxidant properties of gold nanoparticles yielded by a plant extract [27, 28]. The anti-inflammatory, antioxidant and antimicrobial effects of metallic nanoparticles green-synthesized by medicinal plants are well known [28–30]. It also affects a range of molecular targets and signaling pathways, such as NF- κ B, AKT/mTOR, and HIF-1A, and as a result, it plays a role in inhibiting cancer cell proliferation, metastasis, angiogenesis and also inducing apoptosis [30]. Previous studies have also shown that metallic nanoparticles containing medicinal plants cause deformity and perforation of cancer cells, resulting in their death [29, 30].

UV-visible spectroscopy of gold nanoparticles synthesized using *V. thapsus*

UV-Vis is based on the irradiation of ultraviolet and visible photons on the sample and mea-

sures the rate of passage or absorption of matter at different wavelengths in the range of 200 to 1100 nm. It is possible to measure the spectrum for samples in solution, solid as well as thin layers. The size of solid samples should be larger than 20 mm. This test is not possible for powder samples. One of the important applications of the UV device is to determine the concentration of an unknown solution. By having the original sample and its solvent and making several solutions with different percentages and drawing a calibration diagram based on the calculation of the maximum land, the concentration of the unknown solutions can be calculated [14, 15].

UV-Vis spectroscopic analysis showed the presence of an absorption peak at 548 nm which confirmed the formation of the gold nanoparticles (Figure 2). In agreement with our study, Shahriari *et al.* reported *Allium noeanum* Reut. ex Regel aqueous extract synthesized gold nanoparticles with a peak at 542 nm in the UV-visible spectrum [15]. Zhaleh *et al.* reported the absorbance at 528 nm for gold nanoparticles synthesized by *Gundelia tournefortii* L. [14]. Zangneh *et al.* studied *Falcaria vulgaris* aqueous extracts mediated synthesis of gold nanoparticles. Absorption in the spectrum was noted at the wavelength of 535 nm [6]. Hemmati *et al.* reported *Thymus vulgaris* leaf aqueous extract mediated gold nanoparticles and an absorption peak was observed at 532 nm [7]. These reports support the results of the current work.

Transmission electron microscopy analysis of gold nanoparticles synthesized using *V. thapsus*

Transmission electron microscopy (TEM) is used for determining the structure and morphology of

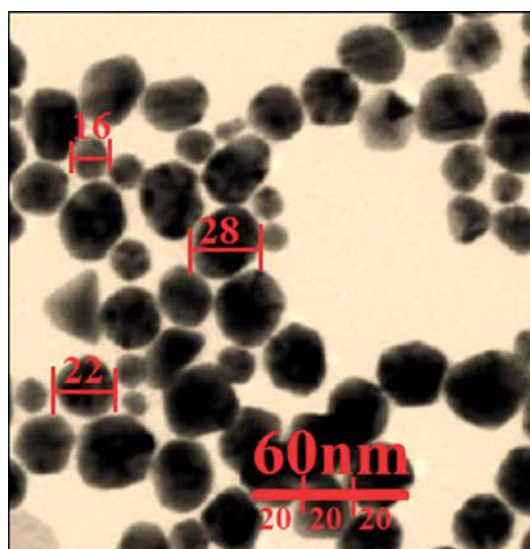


Figure 2. TEM image of gold nanoparticles

materials. TEM enables microstructural studies with high resolution and high magnification such as studies of crystal structures, symmetry, orientation and crystal defects. TEM and SEM microscopes differ in how the beam passes and the information is obtained from the sample. Scanning microscopes take pictures of the sample surface, while passing microscopes take pictures of the inside of the sample. The resolution and magnification of electron microscopes are higher than those of scanning electron microscopes. The electron beams in the scanning electron microscope scan the surface of the sample point-by-point, but the TEM microscope beams hit and pass through the entire sample. In addition, sample preparation for the SEM microscope is easier than for the TEM microscope [14, 15].

TEM is the other test for determining the morphology and size of metallic nanoparticles. In our study, the range size of the nanoparticles (19–24 nm) was calculated through TEM images (Figure 3). Furthermore, the histogram plot from the TEM image showed the particle size distribution of biosynthesized gold nanoparticles in the range of 16 to 22 nm. In previous studies, the size of gold nanoparticles formulated by aqueous extract of medicinal plants had been calculated in the range of 10–45 nm with a spherical shape [6, 7, 14, 15]. These reports support the results of the current work.

FT-IR analysis of gold nanoparticles synthesized using *V. thapsus*

Fourier transform infrared (FT-IR) has been a suitable technique for analyzing materials in the laboratory. An infrared spectrum represents the fingerprint of the sample under test with absorption peaks, which depends on our vibrational frequencies between the atomic bonds of that material. Since each substance has its own atomic bonds, no two compounds with the same infrared spectrum are alike. Hence, infrared spectroscopy can be effective in better identification (qualitative analysis) of different types of materials. Also,

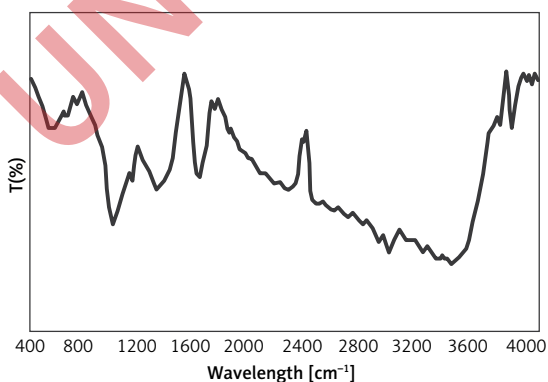


Figure 3. FT-IR spectra of biosynthesized gold nanoparticles

the peak sizes are in the range indicating the amount of material present. Advanced software algorithms make this spectroscopy a great tool for quantitative analysis [14, 15].

In the FT-IR test, the antioxidant and secondary compounds are determined based on several peaks in special wavelengths. The IR spectra investigated for the gold nanoparticles revealed absorption peaks at (I) 3287 cm^{-1} (OH group of alcohols and phenols); (II) 1623 cm^{-1} (C-O group of carboxylic acid group); (III) 1383 cm^{-1} (C=O stretching of carboxylic acid group); (IV) 1038 cm^{-1} (C-OH vibrations of the protein/polysaccharide) [6, 7, 14, 15]. In the present study, the analysis of the IR spectra of the gold nanoparticles revealed peaks at 3473, 1640, 1337, 1086, and 541 cm^{-1} related to OH, C-O, C=O, C-OH, and Au-O respectively (Figure 4).

FE-SEM analysis of gold nanoparticles synthesized using *V. thapsus*

The SEM device is one of the most powerful tools used in various fields, including nanotechnology, which uses electron bombardment to produce images of objects as small as 10 nm. The bombardment of the sample causes positively charged electrons to be released from the sample to the plate, where these electrons become signals [14, 15].

FE-SEM analysis is one of the common chemistry tests for determining the morphology and size of several materials such as metallic nanoparticles. In the present study, the FE-SEM image of gold nanoparticles synthesized using *V. thapsus* leaf aqueous extract is shown in Figure 5. The gold nanoparticles appeared as an agglomerated structure. The hydroxyl groups present in *V. thapsus* could be responsible for agglomeration [31]. Also, FE-SEM images indicated the range size of 16–22 nm and the spherical shape for gold nanoparti-

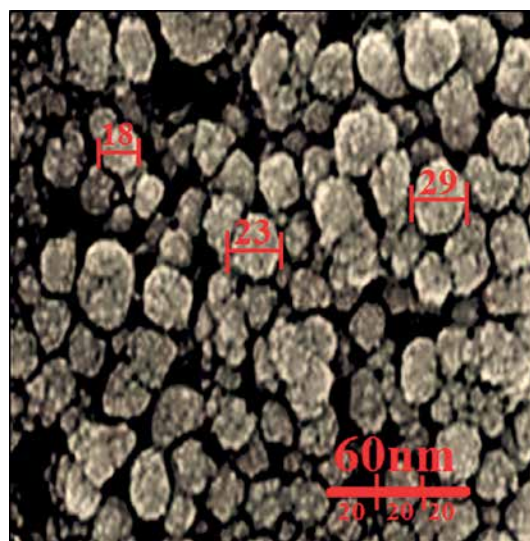


Figure 4. FE-SEM image of gold nanoparticles

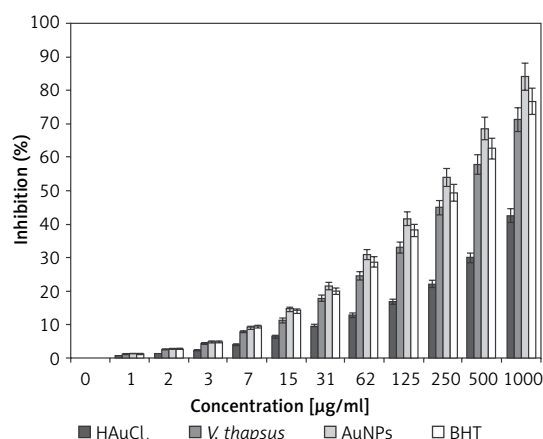


Figure 5. Antioxidant properties of HAuCl₄, *V. thapsus*, AuNPs, and BHT against DPPH

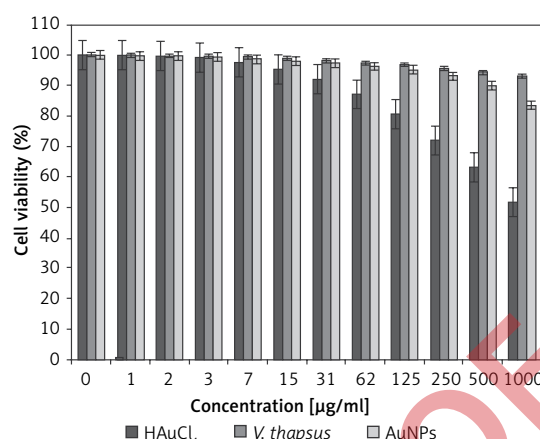


Figure 6. Cytotoxic properties of HAuCl₄, *V. thapsus*, and AuNPs against HUVEC cell line

cles. Many similar observations have been noted by Zhaleh *et al.* [14], Zangneh *et al.* [6], Hemmati *et al.* [7], and Shahriari *et al.* [15].

Antioxidant properties of gold nanoparticles synthesized using *V. thapsus*

Oxidation is the transfer of electrons from an atom and is the aerobic life and metabolism part of living organisms. Oxygen is the receptor for electrons in the electron transport system, which yields energy from adenosine triphosphate (ATP) in the body. Under certain conditions, oxygen may become a single electron and release free radicals. When oxygen becomes a single electron, it is called a reactive oxygen species (ROS). Oxidative loss to proteins, DNA, and other macromolecules is one of the internal causes of degenerative diseases such as aging, cardiovascular disease, cancer, immune system deficiency, cataracts, and abnormal brain function. Single oxygen, high-energy, mutagenic oxygen, can be produced by lipid peroxidation by the transmission of energy from light or the respiratory tract of neutrophils [14, 15]. Some free radicals have positive roles such as regulating cell growth, phagocytosis, energy production, intracellular signals, or the synthesis of important biological compounds. Antioxidants produced in the body fight free radicals with two systems: enzymatic defense and non-enzymatic defense. Superoxide dismutase, catalase, and glutathione peroxidase metabolize lipid peroxide, hydrogen peroxide, and superoxide and prevent the production of toxic hydroxyl radicals [32, 33]. In non-enzymatic defense, there are two classes of antioxidants, fat-soluble (such as carotenoids and vitamin E) and water-soluble (glutathione and vita-

min C), that trap free radicals. These two systems help neutralize oxidants. However, oxidants can escape from antioxidants and damage tissues. In this case, the activated antioxidant repair system (which comprises the enzymes lipase, protease, transferase and DNA repair enzymes) counteracts the oxidant effects. However, due to deficiencies in the production of antioxidants in the body or due to physiopathological factors and situations (such as smoking, air pollution, UV radiation, diets containing high unsaturated fatty acids, inflammation, ischemia, bleeding, etc.) in which ROS are yielded in large quantities at the wrong place and time, oral antioxidants are needed to counteract the cumulative effects of oxidative damage [33–36].

In the present experiment, the antioxidant effects of the gold nanoparticles synthesized using *V. thapsus* leaf aqueous extract were evaluated by DPPH assay, revealing concentration-dependent effects, i.e., an increase in the concentration of the gold nanoparticles leads to an increase in antioxidant activities. In the concentrations studied, the best result was seen in the high concentration or 1000 µg/ml (Figure 6). Comparative analysis of the individual antioxidant assays showed significant variations in the exertion of radical scavenging effects. Among all materials tested (HAuCl₄, *V. thapsus*, and AuNPs), the gold nanoparticles indicated superior inhibitory effects against DPPH. In contrast, standard (butylated hydroxytoluene) demonstrated lower antioxidant effects compared to the gold nanoparticles.

The IC₅₀ values of *V. thapsus*, butylated hydroxytoluene, and AuNPs were 407, 256, and 209 µg/ml, respectively (Table I).

The reason behind the antioxidant activity of green or biosynthesized nanoparticles could be

Table I. IC₅₀ of HAuCl₄, *V. thapsus*, AuNPs, and BHT in the antioxidant test

	HAuCl ₄ [µg/ml]	<i>V. thapsus</i> [µg/ml]	AuNPs [µg/ml]	BHT [µg/ml]
IC ₅₀ against DPPH	–	407	209	256

due to the presence of metabolite compounds such as phenolic compounds, flavonoids, carbohydrates, and other sugar substances [31–36]. Also, many researchers have reported that phenolic and flavonoids attached to the nanoparticles exhibited antioxidant activity. Previously it has been indicated that *V. thapsus* is rich in antioxidant compounds such as β -carotene, lutein, zeaxanthin, cryptoxanthin, triterpene A, triterpene B, saikogenin A, veratric acid, β -spinasterol, 6-O- β -D-xylopyranosyl aucubin, thapsuine B, hydroxythapsuine thapsuine A, 3-O-fucopyranosylsaikogenin F, α -tocopherol, γ -tocopherol, and δ -tocopherol [20]. Several studies have been carried out in the nanotechnology field using various medicinal plants, but still no report is available on gold nanoparticles synthesized using *V. thapsus* leaf aqueous extract.

Cytotoxicity and anti-human lung cancer potential of gold nanoparticles synthesized using *V. thapsus*

Nanotechnology is a new branch of science with a wide range of applications and nanoparticles with different compositions and sizes, shapes and surface chemical properties can have different biological and biomedical applications. Reducing the size of materials at the nanoscale can often cause electrical, magnetic, structural, morphological, and chemical changes. Nanoparticles typically have a higher percentage of atoms on their surface, which increases surface reactions [18]. Proper design of nanomaterials can be used to target specific cancer cells. Nanoparticles have antibacterial and magnetic properties by penetrating microorganisms due to their high surface-to-volume ratio and small size. Also, due to their photocatalytic, catalytic and ionic properties, they are widely used in the fight against human pathogenic microbes, bacteria, fungi and viruses [37–39]. Researchers have shown that gold nanoparticles kill Schwann cells by releasing Au^+ . A study has shown

that concomitant use of gold and doxorubicin reduces the reproductive toxicity of doxorubicin [14, 15]. By producing active bases such as oxygen ions and hydroxides, gold nanoparticles disrupt the metabolism, proliferation and respiration of microorganisms by destroying organic structures and strongly interacting with enzymes and proteins in the electron transfer system, and they can kill more than 650 types of Gram-negative and Gram-positive bacteria resistant to common antibiotics *in vitro* up to 99.9% [37–39]. Metallic nanoparticles in cell cultures and human tissues yield toxins that raise levels of inflammatory products such as cytokines and oxidative stress, ultimately leading to cell death. Larger nanoparticles are seen by the nuclei and mitochondria, causing mutations in DNA, destruction of the mitochondrial structure, and even cell death [40–42]. Solubility and density, surface baroelectricity, surface structure, shape, chemical composition, and size and dimensions are the key factors in determining the toxicity of nanoparticles. The exact effect of gold and gold nanoparticles on cancer cells is not fully understood, but increasing ROS production is one of the possible mechanisms [41, 42]. When nanoparticles are in contact with cancer cells, the cellular defense mechanism is activated to minimize damage. But, if the ROS production stimulation inside the cell by nanoparticles exceeds the cell antioxidant defense capacity, the cells are destroyed during the process of apoptotic cell death [37, 42]. The electrostatic interaction of nanoparticles causes them to be absorbed into target cells. Positively charged nanoparticles are attracted to cancer cells with a high percentage of anionic phospholipids and certain groups of charged proteins and carbohydrates on their outer surface [40–42].

In the present experiment, the treated cells with several concentrations of the present HAuCl_4 , *V. thapsus*, and AuNPs were examined by MTT test for 48 h regarding the cytotoxic properties on normal (HUVEC) and human lung cancer cell lines, i.e., well-differentiated bronchogenic adenocarcinoma (HLC-1), moderately differentiated adenocarcinoma of the lung (LC-2/ad), and poorly differentiated adenocarcinoma of the lung (PC-14) (Figures 7–9; Table II).

The absorbance rate was determined at 570 nm, which indicated extraordinary viability on a normal cell line (HUVEC) even up to 1000 $\mu\text{g}/\text{ml}$ for HAuCl_4 , *V. thapsus*, and AuNPs.

In the case of human lung cancer cell lines, their viability decreased dose-dependently in the presence of HAuCl_4 , *V. thapsus*, and AuNPs. The IC_{50} values of *V. thapsus* and AuNPs against the HLC-1 cell line were 500 and 308 $\mu\text{g}/\text{ml}$, respectively; against the LC-2/ad cell line were 462 and 287 $\mu\text{g}/\text{ml}$, respectively; and against the PC-14 cell line were 396 and 209 $\mu\text{g}/\text{ml}$, respectively.

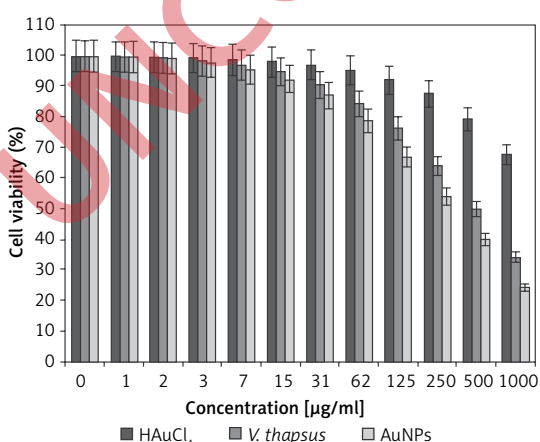


Figure 7. Anti-human lung cancer potential of HAuCl_4 , *V. thapsus*, and AuNPs against well-differentiated bronchogenic adenocarcinoma (HLC-1) cell line

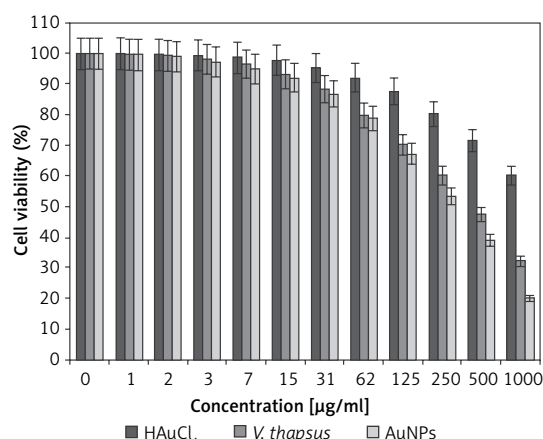


Figure 8. Anti-human lung cancer potential of HAuCl₄, *V. thapsus*, and AuNPs against moderately differentiated adenocarcinoma of the lung (LC-2/ad) cell line

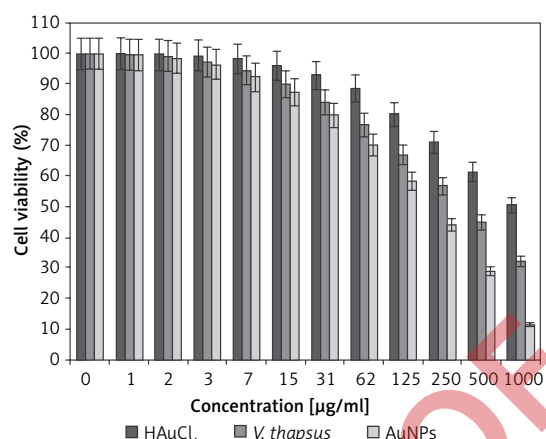


Figure 9. Anti-human lung cancer potential of HAuCl₄, *V. thapsus*, and AuNPs against poorly differentiated adenocarcinoma of the lung (PC-14) cell line

Table II. IC₅₀ of HAuCl₄, *V. thapsus*, and AuNPs in the cytotoxicity test

Variable	HAuCl ₄ [µg/ml]	<i>V. thapsus</i> [µg/ml]	AuNPs [µg/ml]
IC ₅₀ against 'HUVEC'	–	–	–
IC ₅₀ against 'HLC-1'	–	500	308
IC ₅₀ against 'LC-2/ad'	–	462	287
IC ₅₀ against 'PC-14'	–	396	209

The best result of the anti-human lung cancer property of gold nanoparticles against the above cell lines was seen in the case of the poorly differentiated adenocarcinoma of the lung (PC-14) cell line.

Likely the significant anti-human lung cancer potential of gold nanoparticles synthesized by *V. thapsus* leaf aqueous extract against human lung cancer cell lines is linked to their antioxidant activities. Similar studies have revealed that antioxidant materials such as metallic nanoparticles, especially gold nanoparticles and ethno-medicinal plants, reduce the volume of tumors by removing free radicals [39]. In detail, the high presence of free radicals in the normal cells causes many mutation in their DNA and RNA, destroys their gene expression and then accelerates the proliferation and growth of abnormal cells or cancerous cells [40, 41]. The high presence of free radicals in all cancers such as breast, gallbladder, stomach, rectal, liver, gastrointestinal stromal, esophageal, bile duct, small intestine, pancreatic, colon, parathyroid, thyroid, bladder, prostate, testicular, fallopian tube, vaginal, ovarian, hypopharyngeal, throat, lung, and skin cancers indicates the significant role of these molecules in causing angiogenesis and tumorigenesis [41, 42]. Many researchers have reported that gold nanoparticles synthesized by ethno-medicinal plants have a remarkable role in the removing free radicals and growth inhibition of all cancerous cells [38–42].

In conclusion, in the present study, *Verbascum thapsus* L. leaf collected was applied for biosynthesizing gold nanoparticles as a safe and suitable material. After synthesizing gold nanoparticles, they were characterized by TEM, FE-SEM, UV Vis., and FT-IR. The above analyses revealed that gold nanoparticles were synthesized as the best possible form. In the FT-IR test, the presence of many antioxidant compounds with related bonds caused excellent conditions for reduction of gold in the gold nanoparticles, so that the antioxidant properties of gold nanoparticles were better than those of BHT as a positive control. Gold nanoparticles showed significant anti-human lung activities against well-differentiated bronchogenic adenocarcinoma (HLC-1), moderately differentiated adenocarcinoma of the lung (LC-2/ad), and poorly differentiated adenocarcinoma of the lung (PC-14) cell lines. It appears that these nanoparticles may be administered as a chemotherapeutic drug for the treatment of several types of lung cancer, especially well-differentiated bronchogenic adenocarcinoma, moderately differentiated adenocarcinoma of the lung, and poorly differentiated adenocarcinoma of the lung.

Acknowledgments

This project was supported by Researchers Supporting Project number RSP-2021/230, King Saud University, Riyadh, Saudi Arabia.

Means Kaijin Lu and Yan Ou contributed equally to the article.

Conflict of interest

The authors declare no conflict of interest.

References

1. Thun MJ, Hannan LM, Adams-Campbell LL. Lung cancer occurrence in never-smokers: an analysis of 13 cohorts and 22 cancer registry studies. *PLoS Med* 2008; 5: e185.
2. Taylor R, Najafi F, Dobson A. Meta-analysis of studies of passive smoking and lung cancer: effects of study type and continent. *Int J Epidemiol* 2007; 36: 1048-59.
3. Hecht SS. Lung carcinogenesis by tobacco smoke. *Int J Cancer* 2012; 131: 2724-32.
4. Collins LG, Haines C, Perkel R, Enck RE. Lung cancer: diagnosis and management. *Am Fam Physician* 2007; 75: 56-63.
5. Alsharairi NA. The effects of dietary supplements on asthma and lung cancer risk in smokers and non-smokers: a review of the literature. *Nutrient* 2019; 11: 725.
6. Ahmada A, Zangeneh A, Zangeneh MM. Green synthesis and chemical characterization of gold nanoparticle synthesized using *Camellia sinensis* leaf aqueous extract for the treatment of acute myeloid leukemia in comparison to daunorubicin in a leukemic mouse model. *Appl Organometal Chem* 2020; 34: e5290.
7. Hemmati S, Joshani Z, Zangeneh A, Zangeneh MM. *Appl Organometal Chem* 2019; 33: e5267.
8. Raut RW, Kolekar NS, Lakkakula JR, Mendhulkar VD, Kashid SB. *Nano-Micro Lett* 2010; 2: 106.
9. Varma RS. *Curr Opin Chem Eng* 2012; 1: 123.
10. Arunachalam KD, Annamalai SK, S. Hari, *Int J Nanomedicine*. 2003, 8, 1307-1315.
11. L. Sintubin, W. D. Windt, J. Dick, J. Mast, D. van der Ha, W. Verstraete, N. Boon, *Appl Microbiol Biotechnol*. 2009, 6, 741-749.
12. V. Ball, *Front. Bioeng Biotechnol*. 2018, 6, 109.
13. (a) M.M. Zangeneh, *Appl Organometal Chem*. 2019, 33, e5295. DOI:10.1002/aoc.5295. (b) G. Mohammadi, M.M. Zangeneh, A. Zangeneh, Z.M. Siavosh Haghighi, *Appl Organometal Chem*. 2019, 33, e5136. DOI:10.1002/aoc.5136.
14. M. Zhaleh, A. Zangeneh, S. Goorani, N. Seydi, M.M. Zangeneh, R. Tahvilian, E. Pirabbasi, *Appl Organometal Chem*. 2019, 33, e5015.
15. M. Shahrari, S. Hemmati, A. Zangeneh, M.M. Zangeneh, *Appl Organometal Chem*. 2019, 33, e5189. DOI: 10.1002/aoc.5189.
16. M.M. Zangeneh, S. Saneei, A. Zangeneh, R. Tushmalani, A. Haddadi, M. Almasi, A. Amiri Paryan, *Appl Organometal Chem*. 2019, 33, e5216. DOI: 10.1002/aoc.5216.
17. P. Singh, S. Pandit, V. R. S. S. Mokkapati, A. Garg, V. Ravikumar, I. Mijakovic, *Int J Mol Sci*. 2018, 19, 1979.
18. G. Peng, U. Tisch, O. Adams, M. Hakim, N. Shehada, Y.Y. Broza, S. Billan, R. Abdah-Bortnyak, A. Kuten, H. Haick, *Nat Nanotechnol*. 2009, 4, 669-673.
19. A. Soni, R. Krishnamurthy, *Indian J Plant Sci*. 2013, 2, 117-125.
20. M. Riaza, M. Zia-Ul-Haqb, H. Z. E. Jaafar, *Rev Bras Farmacogn*, 2013, 23, 948-959.
21. P. Tveden-Nyborg, T.K. Bergmann, J. Lykkesfeldt, *Basic Clin Pharmacol Toxicol* 2018;123:233-35
22. S.J. Hosseinimehr, A. Mahmoudzadeh, A. Ahmadi, S. A. Ashrafi, N. Shafaghati, N. Hedayati, *Cancer Biother Radiopharm*. 2011, 26, 325-329.
23. V. Arulmozhi, K. Pandian, S. Mirunalini, *Colloids Surf B Biointerfaces*. 2013, 110, 313-320.
24. C. Pereira, A. M. Pereira, C. Fernandes, M. Rocha, R. Mendes, M. P. Fernández-García, A. Guedes, P. B. Tavares, J. M. Grenèche, J. P. Araújo, C. Freire, *Chem Mater*, 2012, 24, 1496-1504.
25. S. P. Deshmukh, S. M. Patil, S. B. Mullani, S. D. Delekar, *Mat Sci Eng C*, 2019, 97, 954-965.
26. A. A. Shah, F. Hasan, A. Hameed, S. Ahmed, *Biotech Adv*, 2008, 26, 246-265.
27. A. E. D. M. van der Heijden, *Chem Eng J*. 2018, 350, 939-948.
28. S. Jin, C. Wu, Z. Zhong Ye, Y. Ying, *Sen Act B Chem*, 2019, 283, 18-34.
29. R. Kumar, A. Umar, G. Kumar, H. S. Salwa, *Ceramics Inter*, 2017, 43, 3940-3961.
30. S. Mehwish, A. Islam, I. Ullah, A. Wakeel, M. Qasim, M. AliKhan, A. Ahmad, N. Ullah, *Biocat Agri Biotech*, 2019, 19, 101117.
31. J. Ramyadevi, K. Jeyasubramanian, A. Marikani, G. Rajakumar, A. A. Rahuman, *Mater Lett*. 2012, 71, 114-116.
32. D. D. Gultekin, A. A. Gungor, H. Onem, A. Babagil, H. Nadaroglu, *J Turk Chem Soc A: Chem*. 2016, 3, 623-36.
33. D. Rehana, D. Mahendiran, R. S. Kumar, A. K. Rahiman, *Biomed Pharmacother*. 2017, 89, 1067-1077.
34. M. Del Mar Delgado-Povedano, V. S. De Medina, J. Bautista, F. Priego-Capote, M. D. De Castro MD, *J Function Foods*. 2016, 24, 403-19.
35. S. C. Jeong, S. R. Koyyalamudi, Y. T. Jeong, C. H. Song, G. Pang, *J Med Food*. 2012, 1, 58-65.
36. R. Sankar, R. Maheswari, S. Karthik, K. S. Shivashangari, V. Ravikumar, *Mat Sci Eng C*. 2014, 44, 234-239.
37. F. Namvar, H.S. Rahman, R. Mohamad, J. Baharara, M. Mahdavi, E. Amini, M.S. Chartrand, S.K. Yeap. *Int J Nanomedicine*. 2014, 19, 2479-88.
38. L. Katata-Seru, T. Moremedi, O.S. Aremu, I. Bahadur, *J Mol Liq*. 2018, 256, 296-304.
39. S. Sangami, B. Manu, *Environ Technol Innov*. 2017, 8, 150-163.
40. N. Beheshtkhoo, M.A.J. Kouhbanani, A. Savardashtaki, A.M. Amani, S. Taghizadeh, *Appl Phys A*. 2018, 124, 363-369.
41. I.A. Radini, N. Hasan, M.A. Malik, Z. Khan, *J Photochem Photobiol B*. 2018, 183, 154-163.
42. G. Oganessian, A. Galstyan, V. Mnatsakanyan, R. Paronikyan, Y.Z. Ter-Zakharyan, *Chem Nat*. 1991, 27, 247-247.